Published in final edited form as:

Curr HIV Res. 2015 ; 13(1): 10–20.

Chronic HIV-1 Tat and HIV Reduce Rbfox3/NeuN: Evidence for Sex-Related Effects

Yun Kyung Hahn[*,1], **Ruturaj R. Masvekar**[1], **Ruqiang Xu**[1], **Kurt F. Hauser**[1,2,3], and **Pamela E. Knapp**[1,2,3]

[1]Department of Anatomy and Neurobiology, Virginia Commonwealth University, Richmond, VA 23298, USA

[2]Department of Pharmacology and Toxicology, Virginia Commonwealth University, Richmond, VA 23298, USA

[3]Institute for Drug and Alcohol Studies, Virginia Commonwealth University, Richmond, VA 23298, USA

Abstract

The NeuN antibody has been widely used to identify and quantify neurons in normal and disease situations based on binding to a nuclear epitope in most types of neurons. This epitope was recently identified as the RNA-binding, feminizing locus on X-3 (Rbfox3), a member of the larger, mammalian Fox1 family of RNA binding proteins. Fox1 proteins recognize a unique UGCAUG mRNA motif and regulate alternative splicing of precursor mRNA to control post-transcriptional events important in neuronal differentiation and central nervous system development. Recent clinical findings show that Rbfox3/NeuN gene dosage is altered in certain human neurodevelopmental disorders, and redistribution has been noted in HIV^+ tissue. We hypothesized that HIV-1 Tat might affect Rbfox3/NeuN expression, and examined this question *in vivo* using inducible transgenic mice, and *in vitro* using human mesencephalic-derived neurons. Rbfox3/NeuN expression and localization in HIV^+ basal ganglia and hippocampus was also examined. Chronic Tat exposure reduced Rbfox3/NeuN protein levels and increased cytoplasmic localization, similar to the effect of HIV exposure. Cytoplasmic Rbfox3/NeuN signal has occasionally been reported, although the meaning or function of cytoplasmic versus nuclear localization remains speculative. Importantly, Rbfox3/NeuN reductions were more significant in male mice. Although Rbfox3/NeuN-expressing cells were significantly decreased by Tat exposure, stereology showed that $Nissl^+$ neuron numbers remained normal. Thus, loss of Rbfox3/NeuN may relate more to functional change than to neuron loss. The effects of Tat by itself are highly relevant to HIV^+ individuals maintained on antiretroviral therapy, since Tat is released from infected cells even when viral replication is inhibited.

[*]Address correspondence to this author at the Department of Anatomy & Neurobiology, MCV Campus, Virginia Commonwealth University, P.O. Box 980709, Richmond, VA 23298-0709, USA; Tel: 804-628-7570; Fax: 804-828-9477; hahnyk@vcu.edu.

CONFLICT OF INTEREST

The authors confirm that this article content has no conflict of interest.

Keywords

Human; male; NeuroAIDS; neurodegeneration; stereology; transgenic

INTRODUCTION

The NeuN antibody, which targets a neuron-specific nuclear protein, has been widely used to quantify normal neurons or to identify the loss of neurons in studies of human immunodeficiency virus (HIV) neuropathogenesis and other disease situations [1–4]. Most CNS neurons, with the exception of cerebellar Purkinje, olfactory bulb mitral, and retinal photoreceptor neurons [4] have been shown to express NeuN. The target of the NeuN antibody was only recently identified as Rbfox3 (RNA-binding, feminizing locus on X-3, or hexaribonucleotide-binding protein 3), a member of the larger mammalian Fox1 family consisting of Rbfox1 (A2BP1), Rbfox2 (Rbm9), and Rbfox3 (NeuN, Hrnbp3). All of these RNA binding proteins recognize the unique mRNA motif, UGCAUG, and regulate alternative splicing of precursor mRNA (pre-mRNA) to control various gene expression and post-transcriptional events important in neuronal differentiation and CNS development [5–10]. There are emerging suggestions that Rbfox3/NeuN may play roles in positive and negative control of proteasome degradation and miRNA biogenesis through non-UGCAUG motif-dependent binding during neuronal development [11, 12].

Even with our increased understanding of Rbfox3/NeuN function, its contributions to the development/differentiation/ maintenance of mammalian neurons remain unclear. There have been suggestions that depletion of Rbfox3/NeuN might signal neuronal injury rather than cell loss [13, 14]. Recent clinical findings show that Rbfox3/NeuN gene dosage was altered in certain human neurodevelopmental disorders [15], and significant redistribution of Rbfox3/NeuN reactivity to the cytoplasm was noted in occipital lobe neurons from HIV-infected individuals with HIV-associated neurocognitive disorders (HAND) compared to uninfected individuals [16]. Cytoplasmic NeuN localization has occasionally been reported in other regions [4, 17], although the meaning or function of cytoplasmic versus nuclear localization remains speculative.

In HIV^+ individuals maintained on antiretroviral therapy, viral proteins such as Tat are released from infected cells even when viral replication is inhibited and may contribute greatly to neurological dysfunction. We thus hypothesized that HIV-1 Tat by itself might affect Rbfox3/NeuN expression, and examined this question *in vivo* using an inducible transgenic mouse, and *in vitro* using human mesencephalic-derived neurons. We also examined Rbfox3/NeuN expression and localization in the basal ganglia and hippocampus of human, HIV^+-tissue samples. We report that Tat by itself affects Rbfox3/NeuN in a manner similar to HIV exposure, and importantly show that the magnitude of this effect is sex-related, being more significant in male mice.

MATERIALS AND METHODS

Experiments were conducted in accordance with procedures reviewed and approved by the Virginia Commonwealth University Institutional Animal Care and Use Committee.

RNA Extraction and Quantitative Real-Time PCR of Human Samples

Frozen human frontal cortex tissues used for qRT-PCR were obtained from the National NeuroAIDS Tissue Consortium (NNTC) Gene Array Project [18, 19] and summarized in Table 1. Briefly, the qRT-PCR project consists of four groups, including HIV-negative (HIV^-), HIV-positive without neurocognitive impairment (HIV^+), HIV-positive with neurocognitive impairment (HIV^+/impair-red), and HIV-positive with combined neurocognitive impairment and HIV encephalitis (HIV^+/impaired/HIVE) (n = 3 for all). All races were included and medically prescribed drugs were allowed. Most of the HIV^+ groups had a history of past and/or current substance abuse, including cannabis, cocaine, opiate, and methadone use. Drug abuse history was not assessed for the HIV^- group. Patients had their first neurological evaluation related to HIV 8–9 years prior to their death. Further details on the subjects and project can be found at https://www.nntc.org/content/gene_array/gene-array-subjects. The details of each group in this study have been previously reported ([20], supplementary data). We only examined samples containing the frontal cortex since other brain regions were available at n < 3. Total RNA in each sample was isolated using the RNeasy Mini Kit (Qiagen, Inc.; Valencia, CA, USA) and used to generate cDNA templates by reverse transcription using the High Capacity cDNA Reverse Transcription Kit (Applied Biosystems; Carlsbad, CA, USA) according to the manufacturer's instructions. Total RNA samples were treated with RNase-free DNase I, then reverse transcribed using the High Capacity cDNA Reverse Transcription Kit (Applied Biosystems). PCR reactions were performed in a total volume of 20 μL containing SensiMix SYBR qPCR reagents (Bioline USA, Inc.; Tauton, MA, USA) using a Corbett Rotor-Gene 6000 real-time PCR system (Qiagen, Inc.). PCR conditions consisted of an initial hold step at 95°C for 10 min followed by 40 amplification cycles of 95°C for 5s, 55°C for 10 s, and 72°C for 20 s. Sequences of the primer sets used were forward: 5′-CAAGCGGCTACACGTCTCC AACAT-3′ and reverse: 5′-GCTCGGTCAGCATCTGAGC TAGT-3′ for Rbfox3/NeuN, and forward: 5′-GCTGCGGTA ATCATGAGGATAAGA-3′ and reverse: 5′-TGAGCACA AGGCCTTCTAACCTTA-3′ for TATA-binding protein (TBP). The specificity of the amplified products was verified by melting curve analysis and agarose gel electrophoresis. qRT-PCR data were calculated as relative expression levels by normalization against TBP mRNA using the $2^{-\Delta\Delta Ct}$ method [21].

Human LUHMES Cell Cultures

Cells of the Lund human mesencephalic cell line (LUHMES; ATCC, Manassas, VA) were grown and differentiated into neurons as described previously [22–24], with minor modifications. In brief, cells were propagated in proliferation medium consisting of Advanced DMEM/F-12 (Gibco, Grand Island, NY), 1X N-2 supplement (Gibco), 2 mM L-glutamine (Gibco), and 40 ng/ml recombinant human basic fibroblast growth factor (bFGF; R&D Systems, Minneapolis, MN), in culture flasks pre-coated with 50 μg/ml poly-L-ornithine (Sigma-Aldrich, St. Louis, MO) and 1 μg/ml fibronectin (3 h at 37°C; Sigma-Aldrich). After cells reached 80% confluency they were detached using pre-warmed 0.025% Trypsin-0.1 g/L EDTA solution (for 3 min at 37°C; Sigma-Aldrich), seeded into 6-well culture plates pre-coated with poly-L-ornithine and fibronectin at a density of 2.0×10^5 cells/well, and placed into proliferation medium. After 24 h, the medium was replaced with differentiation medium consisting of advanced DMEM/F-12, 1X N2 supplement, 2 mM L-

glutamine, 1 mM dibutyryl 3', 5'-cyclic adenosine monophosphate (dibutyryl cAMP; Sigma-Aldrich), 1 μg/ml tetracycline (Sigma-Aldrich), and 2 ng/ml recombinant human glial cell line-derived neurotrophic factor (GDNF; R&D Systems, Minneapolis, MN). All experiments were conducted after 4 d of differentiation when the majority of cells expressed microtubule-associated protein 2 (MAP2), a neuronal marker. All LUHMES-derived neurons were treated with HIV-1 $Tat_{1–86}$ (Clade B; 100 nM; ImmunoDiagnostics, Woburn, MA; heat-inactivated for control) and/or HIV supernatants (25 pg of p24 per treatment) for 48 h. The cells were freshly harvested with ice-cold RIPA buffer (Sigma-Aldrich) with protease inhibitor (cOmplete, Mini, EDTA-free, Roche, Indianapolis, IN) for western blots and the lysates were stored at −80°C until used.

Viral Stock Preparation

A CCR5-preferring strain of HIV ($HIV\text{-}1_{SF162}$) was used to generate infective supernatant, as previously described [25, 26]. Briefly, the U937 human, leukemic, monocytic cell line (ATCC, Manassas, VA) was plated in RPMI-1640 media (Gibco) supplemented with 10% fetal bovine serum (FBS; Gibco), and differentiated/stimulated with 100 ng/ml interleukin-2 (IL-2; Sigma-Aldrich), 5 μg/ml phytohaemagglutinin (PHA; Sigma-Aldrich), and 100 ng/ml phorbol 12-myristate 13-acetate (PMA; Sigma-Aldrich) for 48 h, centrifuged and resuspended in fresh medium, followed by exposure to HIV_{SF162} (p24 = 100 pg/ml; from Dr. Jay Levy [27], through the NIH AIDS Research and Reference Reagent Program, Germantown, MD). Virus was allowed to infect and propagate for 5 d, after which supernatants were collected by filtration through a 0.20-μm filter. HIV infection was verified by quantifying p24 levels in culture supernatants as measured by ELISA (HIV-1 p24 Antigen Capture Assay; Advanced Bioscience Laboratories, Rockville, MD); supernatants were aliquoted and stored at −80°C prior to use. LUHMES cells were grown to 75–80% confluence in 6-well plates before HIV^+ supernatant was added to a final p24 concentration of 25 pg/ml. Viral exposure time was 48 h. Supernatants from uninfected but differentiated U937 cells ($Control_{sup}$) were used as a control.

Animals

Both male and female doxycycline (DOX)-inducible $HIV\text{-}1_{IIIB}$ $Tat_{1–86}$ transgenic mice were generated as described [28–31]. Since the glial fibrillary acidic protein (GFAP) promoter regulates *tat* transgene activity, Tat expression is largely restricted to the CNS. Genotyping was performed in all mice to confirm the presence of *tat* and *rtTA* (Tat^+ mice) or *rtTA* (Tat^- mice) transgenes, as described previously [30]. The chow containing DOX (Harlan Laboratories, Inc., Indianapolis, IN; 6 g/kg) was fed to all groups (both male and female, Tat^- and Tat^+ mice) for three months to induce chronic CNS Tat expression. DOX exposure in Tat^- mice controls for off-target drug effects. Neither the Tat^- or Tat^+ mice showed signs of diarrhea, and weight gain was similar to mice that did not receive DOX [32]. All mice were fed *ad libitum*. Mice were deeply anesthetized with isoflurane (Baxter, Deerfield, IL, USA) prior to perfusion with 4% paraformaldehyde (pH 7.4, Sigma-Aldrich Co., St. Louis, MO) in phosphate-buffered saline (PBS). After perfusion, brains were immediately removed and post-fixed in fresh fixative overnight, hemisected, rinsed several times and left overnight in 15 mL of PBS. Tissues were sectioned at 10 μm (frozen sections for immunohistochemistry) and 50 μm (floating sections for stereology). For cryosections,

the left brain halves were cryopreserved through graded sucrose solutions (10 and 15 %), embedded in Tissue Tek OCT compound (Sacura Finetek, Torrance, CA), and stored at −80°C until use. Coronally sectioned tissues were thaw-mounted on SuperFrost Plus slides (VWR Scientific, West Chester, PA) and processed for immunostaining. The right brain halves were also coronally sectioned at 50 μm as previously described [32]. These tissues were stored in cryoprotectant [30 % sucrose (w/v), 1 % polyvinylpyrrolidone (v/v), 30 % ethylene glycol (v/v) in 0.05 M phosphate buffer, pH 7.2, all from Sigma], at −20 °C until use. Free-floating sections containing the striatum were used for all unbiased stereological estimation. Sectioning was performed with a vibrating blade microtome (Leica VT1200S, Leica, Nussloch, Germany) with ice-cold PBS (Invitrogen) in the reservoir. Sections were thoroughly rinsed and then mounted on gelatin-coated SuperFrost Plus slides (VWR Scientific) in ProLong Gold anti-fade reagent (Life Technologies, Grand Island, NY, USA), and then air-dried for ≥ 8 h in the dark.

Immunohistochemistry - Human Brain Tissue

Paraffin-embedded, human brain tissue sections used for immunohistochemistry were obtained from NNTC subjects outside of the Gene Array Project, details of which are listed in Table 2. Immunohistochemistry was performed on two brain areas (basal ganglia and hippocampus) in each of two HIV groups (uninfected/undisclosed drug abuse history (HIV^-) and HIV-infected with a history of drug abuse (HIV^+). To improve Rbfox3/NeuN immunoreactivity on the paraffin-embedded sections, heat induced antigen retrieval was performed initially, prior to immunostaining for Rbfox3/NeuN. Briefly, paraffin was removed from the tissues with 2–5 min xylene washes, followed by three washes in 2 changes of 100% ethanol for 3 min each, 95% and 80% ethanol for 1 min each, then a rinse in distilled water for rehydration. The slides were immersed in preheated Tris-EDTA buffer (10 mM Tris Base, 1mM EDTA Solution, 0.05% Tween 20, pH 9.0, 95–100°C), and placed into a preheated steamer. The staining dish including slides was incubated for 40 min at 95–100°C. The slides were cooled at room temperature and washed with PBS. After antigen retrieval, human brain sections were permeabilized with 0.2% Triton X-100 in phosphate-buffered saline containing 1% bovine serum albumin (Sigma-Aldrich) for 30 min. Primary antibody directed against Rbfox3/NeuN (1:500, Abcam, Cambridge MA, ab104225) was applied to human brain sections, prior to Hoechst 33342 (1 μg/ml, 8 min, RT; Life Technologies) staining for identification of cell nuclei. Slides were rinsed thoroughly, mounted in ProLong Gold anti-fade reagent (Life Technologies, Grand Island, NY), and then air-dried for ≥ 8 h in the dark.

Immunoblotting

Rbfox3/NeuN proteins from all *in vitro* and animal treatment groups were examined by immunoblotting. All samples for protein extractions were freshly harvested and homogenized (T-PER Reagent, Thermo Scientific, Pittsburgh, PA), including a protease inhibitor cocktail (Roche Applied Science). Homogenized tissue lysates were centrifuged and then stored at −80°C until use. The protein concentration of each sample was measured using the BCA protein assay (Pierce, Rockford, IL). 20 μg of lysates were loaded per well onto 4–20% Tris–HCl Ready Gels (Bio-Rad Laboratories, Hercules, CA) and Precision Plus Protein Dual Color Standards (Bio-Rad; MW range: 10–250 kDa) were used to determine

protein transfer and molecular weight. Proteins were transferred to PVDF membranes (Bio-Rad). Antibodies to Rbfox3/NeuN (1:2,000, Abcam, ab104225) were used to probe the blots. Antibodies to glyceraldehyde 3- phosphate dehydrogenase (GAPDH, 1:2,500, Abcam, ab8245) and β-actin (1:2,000, Abcam, ab8227) were used to normalize protein loading. Host-matched IRDye® Infrared Dyes-conjugated secondary antibodies (LI-COR Biotechnology, Lincoln, Nebraska) were applied to visualize each protein band. Protein bands were detected on an Odyssey® Infrared Imaging System and intensity was analyzed by Odyssey 2.0 software (LI-COR).

Immunohistochemistry and Proportional Quantification in HIV Tat_{1-86} Mouse Model

10 μm frozen sections were permeabilized with 0.2% Triton X-100 in phosphate-buffered saline containing 1% bovine serum albumin (Sigma-Aldrich) for 30 min. Single- or double-label immunostaining was performed in order to assess proportional numbers of neurons in cell cultures or in striata. Primary antibody directed against Rbfox3/NeuN (1:500, Abcam, ab104225) was applied to sections. Primary antibody and host-matched fluorescent-conjugated secondary antibody (Life Technologies, Grand Island, NY, USA) were applied sequentially. Immunostained sections were then incubated with Hoechst 33342 dye (1 μg/ml, 8 min, RT; Life Technologies) to identify nuclei, rinsed thoroughly rinsed, mounted in ProLong Gold anti-fade reagent (Life Technologies), and air-dried for ≥ 8 h in the dark. To verify the proportion of neurons on the coverslips or in the striata, 300–350 $Hoechst^+$ cells were selected randomly within the dorsal striatum and assessed for Rbfox3/NeuN expression, respectively (n = 6). The coverslips and striata were examined under oil immersion at 100× using a Zeiss AxioObserver system with integrated MRM camera system. Multiple patterns of Rbfox3/NeuN expression were detected in the striata of all groups. In most cells within Tat^- brains, immunoreactivity was detected either in the nucleus, or in both nuclear and cytoplasmic locations. However, there were few cells with an entirely cytoplasmic localization in Tat^- brains. In Tat^+ mice, many more cells contained only a cytoplasmic Rbfox3/NeuN signal (Fig. 3F) and very few cells have a strictly nuclear signal. All cells with Rbfox3/NeuN immunoreactivity in the nucleus were counted, including those with only nuclear staining, and those with staining in both the nucleus and cytoplasm (n = 6). Since it is unclear that the ligands for cytoplasmic and nuclear staining are identical, cells with an entirely cytoplasmic staining pattern were not including in cell counts of $Rbfox3/NeuN^+$ cells.

Immunohistochemistry for Cultured Neurons

Cultured LUHMES cells were immunostained using neuron-specific markers including anti-MAP2A/B (1:1000, EMD Millipore, Darmstadt, Germany, MAB378), pan-axonal anti-neurofilament antibody (1: 250, BioLegend, Dedham, MA; SMI-312R), anti-β-tubulin antibody (Abcam, Cambridge, MA, ab108342), mouse monoclonal Rbfox3/ NeuN antibody (1:100, Millipore, MAP377) and rabbit Rbfox3/NeuN antibody (1:500, Abcam, ab104225). For double immunostaining, individual primary antibodies and host-matched fluorescent-conjugated secondary antibodies (Life Technologies) were applied sequentially. All cultured cells on coverslips were stained with Hoechst 33342 dye and mounted in Prolong antifade medium as described above.

Nissl Staining

Nissl staining was used to estimate the total number of neurons in the striatum. Brain tissues were prepared and fixed as described above. Nissl staining was performed on 50 μm brain coronal sections taken serially through the entire striatum. Sectioning was performed with a vibrating blade microtome (Leica VT1200S) with ice-cold PBS (Invitrogen) in the reservoir. Sections were stored in serial order, each in a single well of a 48-well plate with cryoprotectant solution (25% of glycerin: 25% of ethylene glycol: 50% of 0.1 M phosphate buffer) until use. Nissl staining was performed as described [33]. Briefly, free-floating brain sections were mounted serially on chrom-gelatin coated slides and were completely air-dried at room temperature. Brain sections were rehydrated in water for 10 min and then sequentially dehydrated in 70, 95, and 100% ethanol. The brain tissues were stained for 6 min with 0.5% cresyl violet (Sigma–Aldrich). After rinsing in water, the sections were submerged in 70% ethanol in 0.34 M acetic acid for 2–3 sec, and then submerged in 95% ethanol followed by 100% ethanol for 5 min each. Finally, the sections were dehydrated in xylene for 10 min. The sections were mounted and sealed with Permount solution (Fisher Scientific, Pittsburgh, PA) under coverslips for analysis. Nissl histochemical staining has been commonly utilized to quantify the number of neurons in all brain regions in numerous stereological studies [34–37]. Since Nissl staining in brain is seen in both neurons and glia, it was necessary to distinguish between these cell types for accurate cell counting. Neurons were recognized by their larger, pale, and ovoid nuclei surrounded by dark cytoplasmic staining due to a relative high density of Nissl bodies (aggregates of rough endoplasmic reticulum). In contrast, glia, including astrocytes, oligodendro-cytes and microglia, were identified by their relatively smaller sized and comparatively darker or more condensed nuclei, and the much lighter Nissl staining in their cytoplasm [36, 38]. $Nissl^+$ glia identified by these morphological criteria were not considered in the unbiased stereological estimation of total neuron numbers.

Stereology in HIV-1 Tat_{1-86} Transgenic Mice

Brain tissues were prepared and either stained for Nissl substance or immunostained for Rbfox3/NeuN as described above. Unbiased stereological estimations of $Rbfox3/NeuN^+$ cells or $Nissl^+$ neurons in mouse striata were performed as described previously [32]. Briefly, total numbers of stained cells in the striata were estimated using the optical fractionator method [39] with assistance from a computerized stereology system (Stereologer, Systems Planning and Analysis, Alexandria, VA). Every fifth section through the entire striatum was used. A low power objective (5X) was used for outlining each reference space, and cells were then counted using 100X magnification under oil-immersion using a Zeiss AxioObserver system with integrated MRM camera system. (Carl Zeiss, Inc., Thornwood, NY). A guard volume of 2.0 μm was used during cell counting to avoid sectioning artifacts, and counting of repeated or overlapping cells. The criteria for identifying Rbfox3/NeuN-stained cells was identical to that for proportional cell counts; only cells with nuclear staining were counted (n = 4).

Statistical Analysis

Statistical analyses were done by one way and main effect analysis of variance (ANOVA) followed by Duncan's post-hoc testing using Statistica 6.0 software (Statistica, Tulsa, OK). Full statistical details are provided in the individual figure legends. For the LUHMES cell culture studies, each "n" represents an experiment performed on cells from a separate vial using freshly prepared reagents. For studies on tissues or tissue sections, each "n" represents a separate animal.

RESULTS

HIV-1 Infection Reduces Expression of Rbfox3/NeuN mRNA and Protein

Quantitative real-time PCR analyses (qRT-PCR) were conducted to examine expression of mRNAs for Rbfox3/NeuN in human frontal cortex ± frontal lobe white matter samples from the four groups listed in Table 1. Rbfox3/NeuN mRNA levels were significantly decreased as a main effect in HIV-infected groups compared to the HIV^{-}group (Fig. 1A).

We also performed immunohistochemistry to examine whether the expression of Rbfox3/NeuN in human brain tissue was altered by HIV infection. Although Rbfox3/NeuN is considered a nuclear marker, fluorescence that was clearly above background levels was also detected in the cytoplasm of some neurons from brains of both HIV^{+} and HIV^{-} individuals (Fig. 1B). The level of expression in both nuclear and cytoplasmic locations was quite reduced in sections from both the hippocampus and basal ganglia of HIV^{+} individuals compared to similar tissues from HIV^{-} individuals (Fig. 1B). Overall, the results suggested that HIV infection might alter both Rbfox3/NeuN mRNA and protein expression levels within the CNS of HIV infected patients. To determine whether the apparent cytoplasmic localization of Rbfox3/NeuN signal might reflect long post-mortem intervals before tissue harvesting and fixation, we examined staining patterns in cultured human neurons and a murine model.

HIV-1 and HIV-1 Tat Effects on Rbfox3/NeuN Expression in Cultured Human Neurons

To validate toxicity of HIV-1 Tat or HIV on neurons in a more clinically relevant system, we exposed human LUHMES cells differentiated into neurons to HIV-1 $Tat_{1–86}$, or to supernatant from monocytes infected with R5-tropic $HIV\text{-}1_{SF162}$. Before conducting experiments, we briefly characterized the human LUHMES cell line by co-localizing MAP2, pan-axonal neurofilament, β-tubulin, and Rbfox3/ NeuN antigenicity. In accordance with previous reports [22–24], more than 95% of differentiated LUHMES cells expressed MAP2 and Rbfox3/NeuN (Fig. 2A) and approximately 95% also showed pan-axonal neurofilament and β-tubulin immunoreactivity (Fig. 2B, C).

After 48 h exposure to either HIV-1 $Tat_{1–86}$ or HIV^{+}-supernatant, the intensity of Rbfox3/NeuN bands was significantly decreased in immunoblots from cell lysates (Fig. 2D–F). The reduction caused by HIV $Tat_{1–86}$ (100 nM) and HIV^{+}-supernatant (p24 = 25 pg) was between 40–50% loss in both cases, suggesting that exposure to the Tat protein may be a major factor in the effect of HIV virus/supernatant on Rbfox3/NeuN expression.

Interestingly, Rbfox3/NeuN immunostaining was exclusively localized to the nucleus in these cells (Fig. 2). Heat-inactivated Tat had no effect on Rbfox3/NeuN levels (not shown).

Effects of Chronic Tat Induction on Rbfox3/NeuN Expression in HIV-1 Tat Transgenic Mice

Based on our *in vitro* results, we hypothesized that long-term Tat induction might alter the expression level of Rbfox3/NeuN in striata of HIV-1 Tat transgenic mice. We first examined the proportion of Rbfox3/NeuN$^+$ cells in striata of age-matched Tat$^-$ and Tat$^+$ mice of both sexes after 12 weeks of treatment with DOX. In both female and male Tat$^-$ mice, the proportion of total (Hoechst$^+$) cells expressing Rbfox3/NeuN was similar (Fig. 3A). Long-term Tat induction significantly decreased the proportion of Rbfox3/NeuN$^+$ cells in both female and male Tat$^+$ mice compared to their respective controls (Fig. 3A). This result was surprising, based on our earlier studies that striatal neuron numbers were unaffected by Tat [32]. Furthermore, after chronic Tat exposure the Rbfox3/NeuN level was significantly less in males than in females (Fig. 3A). To revalidate the proportional counting, we performed unbiased stereological analysis in all groups. Stereological estimation revealed that genetic sex by itself influenced the total number of Rbfox3/NeuN$^+$ cells in the striatum, which was lower in Tat$^-$ males than in Tat$^-$ females (Fig. 3B). This effect of sex had been observed for total cell numbers in earlier work [32], and was also shown as a main effect in Nissl-stained sections from these same mice (Fig. 3C). Stereological estimation showed a reduction in Rbfox3/NeuN$^+$ cells after Tat exposure, but no effect of sex (Fig. 3B). Results from stereological estimation of Nissl staining were dramatically different, showing absolutely no effect of Tat on numbers of neurons. We reasoned that the reduction of Rbfox3/NeuN$^+$ cells in proportional and stereological counts (Fig. 3A, B), particularly in males, might reflect cells that had fallen below threshold for immunohistochemical detection of NeuN, rather than a true loss of neurons. This hypothesis was partly supported by immunoblot data showing a significant reduction in normalized NeuN levels in male Tat$^+$ mice (Fig. 3D, E). The pattern of Rbfox3/NeuN immunoreactivity in male Tat$^-$ and Tat$^+$ mice was similar to that in the human samples (which were also exclusively males). There were cells with fluorescent signal in the nucleus only, in the cytoplasm only, and in both nucleus and cytoplasm. Cells with only a cytoplasmic signal were visibly increased, and cells with only a nuclear signal were visibly decreased in Tat$^+$ males compared to Tat$^-$ controls (Fig. 3F).

Since the estimated number of immunopositive cells does not necessarily reflect the total amount of protein, we also performed immunoblot analysis to determine if Tat induction affected the Rbfox3/NeuN protein levels in striata. Tat induction significantly reduced the level of Rbfox3/NeuN protein, but only in brains of male mice (Fig. 3A *versus* 3D, F).

DISCUSSION

We report that both HIV and HIV-1 Tat affect the localization and/or tissue levels of Rbfox3/NeuN or mRNA in human and murine brain tissues including the basal ganglia, hippocampus, and striatum, and in isolated human neurons. Our findings show that expression of HIV-1 Tat causes a reduction in Rbfox3/NeuN levels within striatal neurons in the murine brain, and in human-derived neurons in culture. In addition to reducing the overall tissue levels, Tat exposure also alters Rbfox3/NeuN cellular localization. Neurons in

the brains of Tat^{-} mice have a predominantly nuclear localization, while Rbfox3/NeuN appears to be largely cytoplasmic within neurons in Tat^{+} mice. Increased cytoplasmic localization of Rbfox3/NeuN was also seen in the hippocampus and basal ganglia of human HIV^{+} individuals, in which we also found lower levels of Rbfox3/NeuN mRNA as a main effect of HIV. Lucas *et al*. [16] reported similar localization of Rbfox3/NeuN in occipital lobe neurons from HIV-infected post-mortem samples. Given these consistent results, it was surprising that exposure to Tat or to HIV^{+}-supernatant did not alter the localization of Rbfox3/NeuN in cultured human mesencephalic neurons, even though both treatments significantly reduced protein levels (Fig. 2). Since cultures were only exposed to Tat or HIV for 48 h, this suggests that redistribution of NeuN to the cytoplasmic compartment might be related to a more chronic Tat or HIV exposure, or to changes in the milieu within the brain. Cultured neurons are also relatively immature, and Rbfox3/NeuN nuclear localization/signal strength appears to decrease with age [40]. The brain region or neuron type sampled is another variable that must be considered. Commercially obtained mesencephalic neurons were well-differentiated and robust, and were used in preference to cortical cells from commercial vendors that appeared to contain many interneurons. Tissues that are available from control and HIV^{+} brains from NNTC are limited, and comparisons between exact brain regions, sample numbers, or matched for the use of abused drugs and other parameters, often cannot be made. Our samples were well-matched for disease duration, all samples were from males, and all HIV^{+} individuals had a history of drug abuse although the mixture of drugs cannot be truly ascertained. However, we were unable to match brain region samples for PCR and immunostaining. PCR results are from frontal cortex/frontal lobe including white matter, while immunostaining was done on basal ganglia and hippocampus. Even given these variables, many outcomes of this study were quite similar between human and murine samples.

The finding that Rbfox3/NeuN levels and localization are similarly altered in HIV-1 Tat transgenic and human HIV^{+} tissue suggests several things. Firstly, the changes in HIV^{+} brain are unlikely an artifact due to long postmortem intervals since they also occur in the mice. In addition, the results suggest that much of the effect in the patient tissue may be due to the effects of Tat.

Because of increasing evidence that there may be differential neural/CNS deficits due to biological sex in HIV^{+} humans [41–45] and experimental animal models [32], we examined Rbfox3/NeuN in both male and female Tat transgenic mice. In female mice, immunoblots showed no significant change in levels of NeuN in Tat^{+} versus control mice, and levels were also similar to those in male control mice (Fig. 3D, E). However, in the Tat^{+} male mice, the level of Rbfox3/NeuN protein was reduced quite significantly. Regulation of Rbfox3/NeuN levels thus differs between sexes such that males are more vulnerable to the effects of Tat. We previously observed an increased propensity for males to be affected by Tat exposure in terms of microglial activation, astrogliosis, and certain behaviors [32]. Unfortunately, as all human samples available to us were from males, the existence of a similar sex-related difference could not be ascertained for HIV-infected patients. In an earlier report of NeuN redistribution in HIV^{+} occipital lobe the samples, with one exception, were also all males [16]. If males are more vulnerable to aspects of HIV neuropathology, this would be similar

to other CNS situations such as trauma and Parkinson's disease where both epidemiological and experimental data suggest that outcomes in males are worse [46–48]. Although the reasons for enhanced Tat effects in males were not explored in our study, they might be due to the absence of female sex hormones, which have been suggested to be neuroprotective in other situations.

Importantly, stereological analysis of Nissl staining in Tat transgenic mice showed that the total numbers of neurons were maintained at a normal level in both males and females, even when total Rbfox3/NeuN$^+$ cells or protein declined. This is similar to our previous findings that neuron-specific enolase$^+$ numbers were unaffected by chronic HIV-1 Tat exposure *in vivo* [32]. Un-induced female mice had more total neurons, and more Rbfox3/NeuN$^+$ cells than did male mice (Fig. 3A–C), but this basal difference in neuron numbers between sexes is not surprising as we previously showed that female striata contain higher numbers of total cells. The finding that male Tat$^+$ mice show more of a decline in the proportion of total cells that express Rbfox3/NeuN than females (Fig. 3A) was initially a bit puzzling. However, as only the males showed a reduction in total Rbfox3/NeuN protein, the explanation might be that fewer neurons in males have sufficient cellular Rbfox3/NeuN to reach the threshold detectable by immunohistochemistry. Another explanation might lie in our criteria for identifying Rbfox3/NeuN$^+$ cells. Rbfox3/NeuN is usually found within neuronal nuclei, and the identity/source of the signal detected in the cytoplasm remains unclear. For this reason, we only counted cells in which a nuclear signal was evident, regardless of whether there was any reaction product within the cytoplasm. If the cytoplasmic signal truly is Rbfox3/NeuN that has been redistributed, and not signal due to a cross-reacting protein such as Synapsin I [9], then the overall amount of Rbfox3/NeuN might remain the same even though a decreased percentage of cells with nuclear Rbfox3/NeuN is counted. Differential subcellular localization may reflect alternative splicing of terminal Rbfox3/NeuN exons with nuclear export or nuclear localization signals, or phosphorylation-dependent antigenicity [49]. Expression of such Rbfox3/NeuN variants in HeLa cells does affect relative levels of nuclear versus cytoplasmic signal [50]. The role of Rbfox3/NeuN in maintaining or reflecting neuron function is still uncertain. It has been noted that Rbfox3/NeuN immunoreactivity in cerebellar neurons is reduced with chronic depolarization [51] and that Rbfox3/NeuN antigenicity can be lost in the aging spinal cord [40]. Findings such as these suggest that Rbfox3/NeuN levels may be indicative of a wide range of neuropathologic situations, or perhaps that changes in Rbfox3/NeuN-regulated splicing may underlie neuropathogenic processes. As HIV does not infect neurons, the altered expression of Rbfox3/NeuN in HIV$^+$ brain tissue is most likely due to exposure to Tat protein and/or other effects of the inflammatory milieu. The finding that Tat causes changes in Rbfox3/NeuN expression that are similar to those of HIV exposure or infection is noteworthy. Tat is produced by infected cells even when viral replication is held in check by antiretroviral treatments, and Tat can be detected in the CSF and brain of HIV-infected persons, even in the absence of detectable viral replication [52]. As the longevity of individuals living with HIV infection continues to increase, effects of HIV Tat protein on brain function may become an increasing determinant of the characteristics of HIV-associated neurological disease.

ACKNOWLEDGEMENTS

This work was supported by funding from NIH | National Institute on Drug Abuse (NIDA) - DA034231 [Knapp/Hauser]; DA024461 [Knapp]. The funders had no role in study design, data collection and analysis, decision to publish, or preparation of the manuscript.

Biography

Yun Kyung Hahn

ABBREVIATIONS

A2BP1	Ataxin 2-binding protein 1
ANOVA	Analysis of variance
bFGF	Basic fibroblast growth factor
cDNA	Complementary deoxyribonucleic acid
CSF	Cerebrospinal fluid
dibutyryl cAMP	Dibutyryl 3’, 5’-cyclic adenosine monophosphate
DMEM	Dulbecco’s Modified Eagle’s Medium
DOX	Doxycycline
EDTA	Ethylenediaminetetraacetic acid
ELISA	Enzyme-linked immunosorbent assay
FBS	Fetal bovine serum
GAPDH	Glyceraldehyde 3-phosphate dehydrogenase
GDNF	Glial cell derived neurotropic factor
GFAP	Glial fibrillary acidic protein
HIV-1	Human immunodeficiency virus type 1
HIV-1$_{SF162}$	An M-tropic strain of HIV
HIVE	Human immunodeficiency virus type 1 encephalitis
IL-2	Interleukin-2
LUHMES	Lund human mesencephalic cell line
MAP2	Microtubule-associated protein 2
MCMD	Mild cognitive motor deficit

NeuN	Neuronal Nuclei
NNTC	National NeuroAIDS Tissue Consortium
PBS	Phosphate-buffered saline
PCR	Polymerase chain reaction
PHA	Phytohaemagglutinin
PMA	Phorbol 12-myristate 13-acetate
PVDF	Polyvinylidene fluoride
qRT-PCR	Quantitative real-time PCR
Rbfox3	RNA-binding, feminizing locus on X-3, or hexaribonucleotide-binding protein 3
Rbm9	RNA binding motif protein 9
RIPA buffer	Radioimmunoprecipitation assay buffer
RNA	Ribonucleic acid
RPMI-1640 media	Roswell Park Memorial Institute-1640 media
rtTA	Reverse tetracycline transactivator
SEM	Standard error of the mean
TBP	TATA-binding protein

REFERENCES

1. Everall IP, Bell C, Mallory M, et al. Lithium ameliorates HIV- gp120-mediated neurotoxicity. Mol Cell Neurosci. 2002; 21:493–501. [PubMed: 12498789]
2. Zujovic V, Benavides J, Vige X, Carter C, Taupin V. Fractalkine modulates TNF-alpha secretion and neurotoxicity induced by microglial activation. Glia. 2000; 29:305–315. [PubMed: 10652441]
3. Dou H, Birusingh K, Faraci J, et al. Neuroprotective activities of sodium valproate in a murine model of human immunodeficiency virus-1 encephalitis. J Neurosci. 2003; 23:9162–9170. [PubMed: 14534250]
4. Mullen RJ, Buck CR, Smith AM. NeuN, a neuronal specific nuclear protein in vertebrates. Development. 1992; 116:201–211. [PubMed: 1483388]
5. Jin Y, Suzuki H, Maegawa S, et al. A vertebrate RNA-binding protein Fox-1 regulates tissue-specific splicing *via* the pentanucleotide GCAUG. EMBO J. 2003; 22:905–912. [PubMed: 12574126]
6. Nakahata S, Kawamoto S. Tissue-dependent isoforms of mammalian Fox-1 homologs are associated with tissue-specific splicing activities. Nucleic Acids Res. 2005; 33(7):2078–2089. [PubMed: 15824060]
7. Ponthier JL, Schluepen C, Chen W, et al. Fox-2 splicing factor binds to a conserved intron motif to promote inclusion of protein 4.1R alternative exon 16. J Biol Chem. 2006; 281:12468–12474. [PubMed: 16537540]
8. Underwood JG, Boutz PL, Dougherty JD, Stoilov P, Black DL. Homologues of the Caenorhabditis elegans Fox-1 protein are neuronal splicing regulators in mammals. Mol Cell Biol. 2005; 25:10005–10016. [PubMed: 16260614]

9. Kim KK, Adelstein RS, Kawamoto S. Identification of neuronal nuclei (NeuN) as Fox-3, a new member of the Fox-1 gene family of splicing factors. J Biol Chem. 2009; 284:31052–31061. [PubMed: 19713214]
10. Kim KK, Nam J, Mukouyama YS, Kawamoto S. Rbfox3-regulated alternative splicing of Numb promotes neuronal differentiation during development. J Cell Biol. 2013; 200:443–458. [PubMed: 23420872]
11. Kim KK, Yang Y, Zhu J, Adelstein RS, Kawamoto S. Rbfox3 controls the biogenesis of a subset of microRNAs. Nat Stru & Mol Biol. 2014; 21:901–910.
12. Kim KK, Adelstein RS, Kawamoto S. Isoform-specific proteasomal degradation of Rbfox3 during chicken embryonic development. Biochem & Biophysi Res Commu. 2014; 450:1662–1667.
13. Unal-Cevik I, Kilinc M, Gursoy-Ozdemir Y, Gurer G, Dalkara T. Loss of NeuN immunoreactivity after cerebral ischemia does not indicate neuronal cell loss: a cautionary note. Brain Res. 2004; 1015:169–174. [PubMed: 15223381]
14. Collombet JM, Masqueliez C, Four E, et al. Early reduction of NeuN antigenicity induced by soman poisoning in mice can be used to predict delayed neuronal degeneration in the hippocampus. Neurosci Lett. 2006; 398:337–342. [PubMed: 16472911]
15. Utami KH, Hillmer AM, Aksoy I, et al. Detection of chromosomal breakpoints in patients with developmental delay and speech disorders. PLoS ONE. 2014; 9:e90852. [PubMed: 24603971]
16. Lucas CH, Calvez M, Babu R, Brown A. Altered subcellular localization of the NeuN/Rbfox3 RNA splicing factor in HIV-associated neurocognitive disorders (HAND). Neurosci Lett. 2014; 558:97–102. [PubMed: 24215932]
17. Van Nassauw L, Wu M, De Jonge F, Adriaensen D, Timmermans JP. Cytoplasmic, but not nuclear, expression of the neuronal nuclei (NeuN) antibody is an exclusive feature of Dogiel type II neurons in the guinea-pig gastrointestinal tract. Histochem and Cell Biol. 2005; 124:369–377. [PubMed: 16049694]
18. Gelman BB, Chen T, Lisinicchia JG, et al. The National NeuroAIDS Tissue Consortium brain gene array: two types of HIV-associated neurocognitive impairment. PLoS ONE. 2012; 7:e46178. [PubMed: 23049970]
19. Morgello S, Gelman BB, Kozlowski PB, et al. The National NeuroAIDS Tissue Consortium: a new paradigm in brain banking with an emphasis on infectious disease. Neuropath Appl Neuro. 2001; 27:326–335.
20. Dever SM, Xu R, Fitting S, Knapp PE, Hauser KF. Differential expression and HIV-1 regulation of mu-opioid receptor splice variants across human central nervous system cell types. J Neurovirol. 2012; 18:181–190. [PubMed: 22528479]
21. Livak KJ, Schmittgen TD. Analysis of relative gene expression data using real-time quantitative PCR and the 2(–Delta Delta C(T)) Method. Methods. 2001; 25:402–408. [PubMed: 11846609]
22. Schildknecht S, Poltl D, Nagel DM, et al. Requirement of a dopaminergic neuronal phenotype for toxicity of low concentrations of 1-methyl-4-phenylpyridinium to human cells. Toxicol Appl Pharm. 2009; 241:23–35.
23. Scholz D, Poltl D, Genewsky A, et al. Rapid, complete and large-scale generation of post-mitotic neurons from the human LUHMES cell line. J Neurochem. 2011; 119:957–971. [PubMed: 21434924]
24. Lotharius J, Falsig J, van Beek J, et al. Progressive degeneration of human mesencephalic neuron-derived cells triggered by dopamine- dependent oxidative stress is dependent on the mixed-lineage kinase pathway. J Neurosci. 2005; 25:6329–6342. [PubMed: 16000623]
25. Masvekar RR, El-Hage N, Hauser KF, Knapp PE. Morphine enhances HIV-1SF162-mediated neuron death and delays recovery of injured neurites. PLoS ONE. 2014; 9:e100196. [PubMed: 24949623]
26. Hahn YK, Podhaizer EM, Hauser KF, Knapp PE. HIV-1 alters neural and glial progenitor cell dynamics in the central nervous system: Coordinated response to opiates during maturation. Glia. 2012; 60:1871–1887. [PubMed: 22865725]
27. Cheng-Mayer C, Levy JA. Distinct biological and serological properties of human immunodeficiency viruses from the brain. Ann Neurol. 1988; (23 Suppl):S58–S61. [PubMed: 3258140]

28. Hauser KF, Hahn YK, Adjan VV, Zou S, Buch SK, Nath A, et al. HIV-1 Tat and morphine have interactive effects on oligodendrocyte survival and morphology. Glia. 2009; 57:194–206. [PubMed: 18756534]
29. Fitting S, Xu R, Bull C, et al. Interactive comorbidity between opioid drug abuse and HIV-1 Tat: chronic exposure augments spine loss and sublethal dendritic pathology in striatal neurons. Am J Pathol. 2010; 177:1397–1410. [PubMed: 20651230]
30. Bruce-Keller AJ, Turchan-Cholewo J, Smart EJ, et al. Morphine causes rapid increases in glial activation and neuronal injury in the striatum of inducible HIV-1 tat transgenic mice. Glia. 2008; 56:1414–1427. [PubMed: 18551626]
31. Fitting S, Ignatowska-Jankowska BM, Bull C, et al. Synaptic Dysfunction in the Hippocampus Accompanies Learning and Memory Deficits in Human Immunodeficiency Virus Type 1 Transactivator of Transcription Transgenic Mice. Biol Psychiat. 2013; 73:443–453. [PubMed: 23218253]
32. Hahn YK, Podhaizer EM, Farris SP, et al. Effects of chronic HIV-1 Tat exposure in the CNS: heightened vulnerability of males versus females to changes in cell numbers, synaptic integrity, and behavior. Brain Struc Funct. 2015 in press.
33. Davenport HA. Histological and Histochemical Techniques. 1960
34. Nielsen MS, Sorensen JC, Bjarkam CR. The substantia nigra pars compacta of the Gottingen minipig: an anatomical and stereological study. Brain Struc Funct. 2009; 213:481–488.
35. Fitting S, Booze RM, Mactutus CF. Neonatal intrahippocampal injection of the HIV-1 proteins gp120 and Tat: differential effects on behavior and the relationship to stereological hippocampal measures. Brain Res. 2008; 1232:139–154. [PubMed: 18674522]
36. Fitting S, Booze RM, Hasselrot U, Mactutus CF. Dose-dependent long-term effects of Tat in the rat hippocampal formation: a design-based stereological study. Hippocampus. 2010; 20:469–480. [PubMed: 19489004]
37. Cyr M, Caron MG, Johnson GA, Laakso A. Magnetic resonance imaging at microscopic resolution reveals subtle morphological changes in a mouse model of dopaminergic hyperfunction. Neuroimage. 2005; 26:83–90. [PubMed: 15862208]
38. Sherwood CC, Stimpson CD, Raghanti MA, et al. Evolution of increased glia-neuron ratios in the human frontal cortex. Proc Natl Acad Sci USA. 2006; 103:13606–13611. [PubMed: 16938869]
39. Mouton, PR. Baltimore: Johns Hopkins University Press; 2002. Principles and practices of unbiased stereology : an introduction for bioscientists; p. 214x
40. Portiansky EL, Barbeito CG, Gimeno EJ, Zuccolilli GO, Goya RG. Loss of NeuN immunoreactivity in rat spinal cord neurons during aging. Exp Neurol. 2006; 202:519–521. [PubMed: 16935281]
41. Wojna V, Skolasky RL, Hechavarria R, et al. Prevalence of human immunodeficiency virus-associated cognitive impairment in a group of Hispanic women at risk for neurological impairment. J Neurovirol. 2006; 12:356–364. [PubMed: 17065128]
42. Gupta JD, Satishchandra P, Gopukumar K, et al. Neuropsychological deficits in human immunodeficiency virus type 1 clade C-seropositive adults from South India. J Neurovirol. 2007; 13:195–202. [PubMed: 17613709]
43. Hestad KA, Menon JA, Silalukey-Ngoma M, et al. Sex differences in neuropsychological performance as an effect of human immunodeficiency virus infection: a pilot study in Zambia, Africa. J Nerv Ment Dis. 2012; 200:336–342. [PubMed: 22456588]
44. Joska JA, Westgarth-Taylor J, Myer L, et al. Characterization of HIV-Associated Neurocognitive Disorders among individuals starting antiretroviral therapy in South Africa. AIDS Behav. 2011; 15:1197–1203. [PubMed: 20614176]
45. Lopes M, Olfson M, Rabkin J, et al. Gender, HIV status, and psychiatric disorders: results from the National Epidemiologic Survey on Alcohol and Related Conditions. J Clin Psychiatry. 2012; 73:384–391. [PubMed: 22053858]
46. de Lau LM, Breteler MM. Epidemiology of Parkinson's disease. Lancet Neurol. 2006; 5:525–535. [PubMed: 16713924]
47. Van Den Eeden SK, Tanner CM, Bernstein AL, et al. Incidence of Parkinson's disease: variation by age, gender, and race/ethnicity. Am J Epidemiol. 2003; 157:1015–1022. [PubMed: 12777365]

48. Coronado VG, Xu L, Basavaraju SV, et al. Surveillance for traumatic brain injury-related deaths--United States, 1997–2007. MMWR Surveill Summ. 2011; 60:1–32. [PubMed: 21544045]

49. Maxeiner S, Glassmann A, Kao HT, Schilling K. The molecular basis of the specificity and cross-reactivity of the NeuN epitope of the neuron-specific splicing regulator, Rbfox3. Histochem Cell Biol. 2014; 141:43–55. [PubMed: 24150744]

50. Dredge BK, Jensen KB. NeuN/Rbfox3 nuclear and cytoplasmic isoforms differentially regulate alternative splicing and nonsense-mediated decay of Rbfox2. PLoS ONE. 2011; 6:e21585. [PubMed: 21747913]

51. Weyer A, Schilling K. Developmental and cell type-specific expression of the neuronal marker NeuN in the murine cerebellum. J Neurosci Res. 2003; 73:400–409. [PubMed: 12868073]

52. Johnson TP, Patel K, Johnson KR, et al. Induction of IL-17 and nonclassical T-cell activation by HIV-Tat protein. Proc Natl Acad Sci USA. 2013; 110:13588–13593. [PubMed: 23898208]

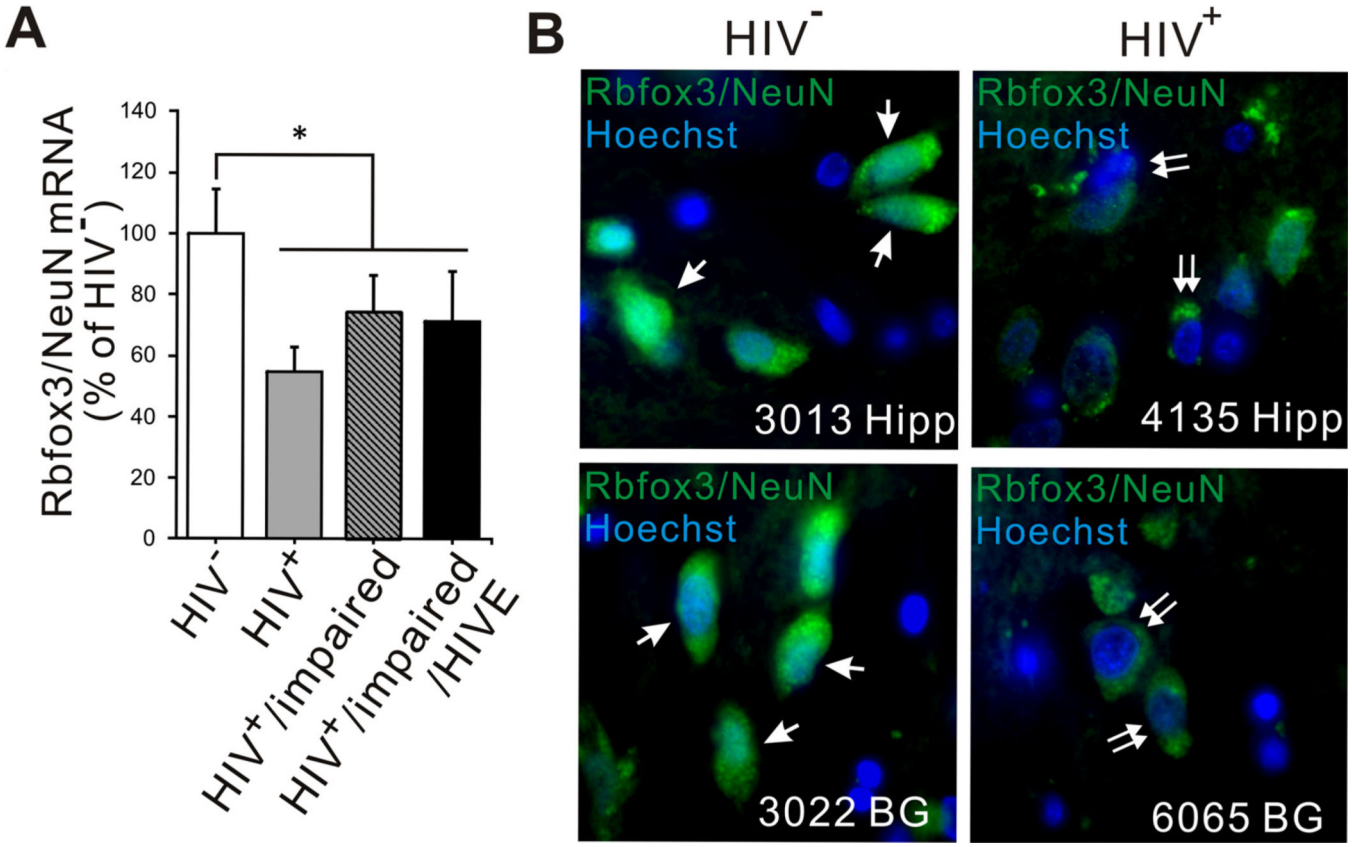

Fig. (1).

qPCR analysis of Rbfox3/NeuN mRNA expression and immunohistochemistry in HIV-1-infected human brain tissue. (**A**) qPCR was performed to examine expression level of Rbfox3/NeuN mRNA in frontal lobe/frontal cortex in the four groups detailed in Table 1. Rbfox3/NeuN mRNA expression was significantly reduced in all HIV infected groups (HIV^+, HIV^+/impaired, HIV^+/impaired/HIVE) compared to the uninfected group (HIV). Expression levels were determined by normalization to TBP mRNA and presented as compared with levels in HIV samples, which were considered to be 100%. Error bars show SEM [n = 3; one-way ANOVA, main effect of HIV*vs* all HIV^+ groups: $F(1,10) = 5.17$, $p = 0.049$, $^*p < 0.05$]. There was no significant difference among HIV infected groups in Rbfox3/NeuN mRNA expression. (**B**) Rbfox3/NeuN immunohistochemistry was performed on basal ganglia (BG) and hippocampus (Hipp) tissues from HIV^+ and HIV individuals for revalidation of qPCR data. All sections were stained at the same time and scanned at the same laser settings so that staining and visualization were internally consistent. The intensity of overall fluorescence is considerably lower in the HIV^+ tissues. Additionally, HIV^+ sections from both basal ganglia and hippocampus have fewer Rbfox3/$NeuN^+$ cells with nuclear localization (arrow) and more cells with entirely cytoplasmic localization (double arrow).

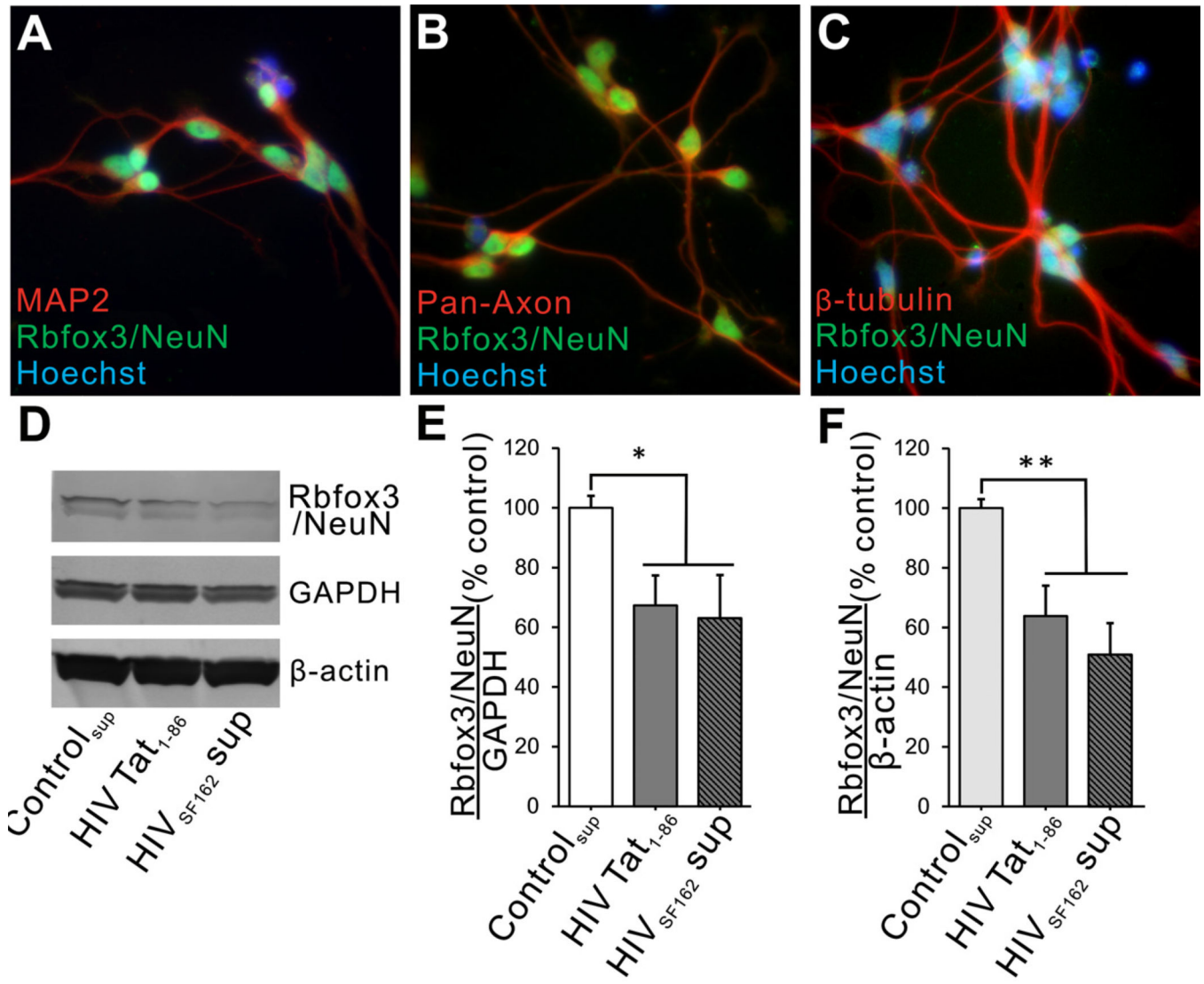

Fig. (2).

Effects of HIV-1 Tat protein and HIV$^+$ supernatant on differentiated human LUHMES cells. (**A–C**) Immunohistochemistry was performed with multiple neuron-specific markers and anti-Rbfox3/NeuN antibody on differentiated LUHMES cells prior to treatments. In addition to having nuclear Rbfox3/NeuN immunostaining, >95% LUHMES cells showed immunoreactivity with antibodies to MAP2, pan-axonal neurofilaments, and β-tubulin. (**D–F**) LUHMES cells were treated with HIV-1 $Tat_{1–86}$ or HIV_{SF162} supernatant for 48 h. Immunoblots showed that both Tat and HIV exposure decreased Rbfox3/NeuN protein levels when normalized to GAPDH. To ensure that this decrease was not an artifact of changing GAPDH levels, we also normalized to β-actin and the results were similar (Fig. 2**E**: n = 4; one-way ANOVA, Duncan post hoc test, $F(2, 9) = 7.65$, $p = 0.049$, $^*p < 0.05$; Fig. 2**F**: n = 4; one-way ANOVA, Duncan post hoc test, $F(2, 9) = 9.07$, $p = 0.006$, $p^{**} < 0.01$).

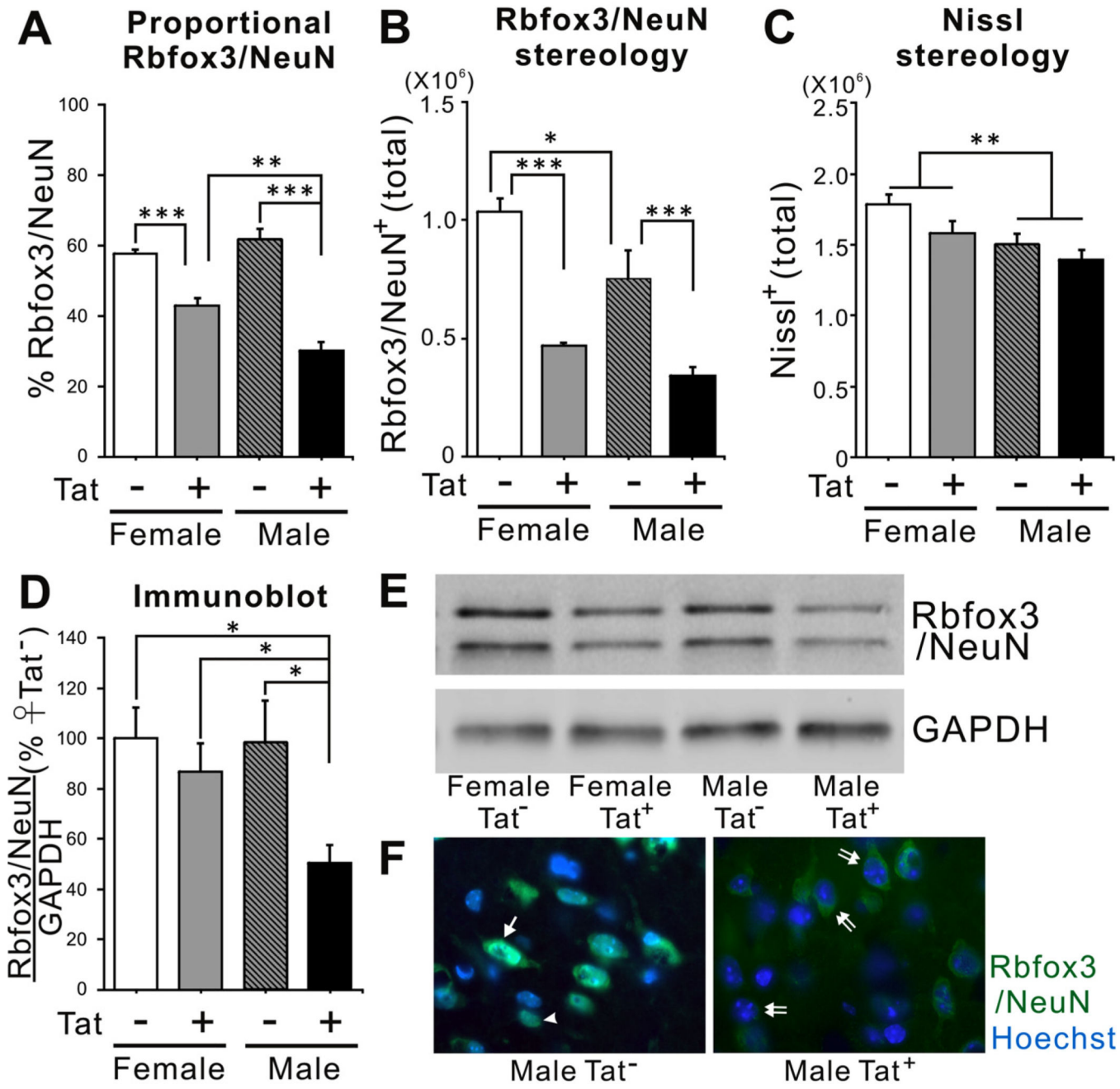

Fig. (3).

Effects of chronic Tat induction on expression of Rbfox3/NeuN in the striatum of HIV-1 Tat transgenic male and female mice. (**A**) Chronic Tat expression decreased the proportion of Rbfox3/NeuN$^+$ cells in the striatum of both sexes. The percentage of Rbfox3/NeuN $^+$ cells in male Tat$^+$ striata was significantly lower than was observed in female Tat$^+$ striata [n = 6; one-way ANOVA, Duncan post hoc test, F(3, 20) = 39.72, p = 0.0001 p** < 0.01, p*** < 0.001]. (**B**) Unbiased stereological estimation indicated that there were fewer Rbfox3/NeuN $^+$ cells in Tat males than Tat females. Tat induction significantly decreased Rbfox3/NeuN$^+$ cells in the striata of both male and female Tat$^+$ mice to a similar degree [n = 3; one-

way ANOVA, Duncan post hoc test, $F(2, 8) = 21.84$, $p = 0.0003$, * $p<0.05$, ***$p<0.001$]. (**C**) Unbiased stereological estimation showed that total $Nissl^+$ neurons were higher in female mice than in male mice [n = 3; one-way ANOVA, main effect, $F(3, 8) = 5.23$, $p = 0.027$, * $p<0.05$]. There was no effect of chronic Tat exposure on total $Nissl^+$ neurons in either male or female mice. (**D, E**) Striatal lysates from all groups were examined by immunoblotting to compare striatal Rbfox3/NeuN protein. Rbfox3/NeuN protein was significantly decreased only in male Tat^+ mice [n = 6; one-way ANOVA, Duncan post hoc test, $F(3, 16) = 4.58$, $p = 0.020$, * $p<0.05$]. (**F**) Rbfox3/NeuN immunohistochemistry in the striatum of Tat and Tat^+ male mice induced with DOX. Overall, Tat^+ males showed a greatly reduced level of Rbfox3/NeuN staining intensity. The percentage of cells in Tat^+ mice that have nuclear Rbfox3/NeuN was reduced, while the percentage with entirely cytoplasmic signal was increased (arrowhead indicates signal entirely in the nucleus; single arrow indicates both nuclear and cytoplasmic signal; double arrow indicates signal entirely in the cytoplasm).

Table 1

Human brain tissue samples used for qRT-PCR*.

Gene Array ID	HIV Status/Impairment Status	NNTC ID	Sample Origin
A4	HIV/impairment unknown	7101727068	Combined frontal lobe white matter/frontal cortex
A5	HIV/impairment unknown	7101198377	Combined frontal lobe white matter/frontal cortex
A6	HIV/impairment unknown	CA244	Frontal cortex
B2	HIV^+/not impaired	7100246771	Combined frontal lobe white matter/frontal cortex
B3	HIV^+/not impaired	7200267172	Combined frontal lobe white matter/frontal cortex
B6	HIV^+/not impaired	6052	Frontal cortex
C2	HIV^+/impaired	7200116866	Combined frontal lobe white matter/frontal cortex
C3	HIV^+/impaired	7200537480	Combined frontal lobe white matter/frontal cortex
C7	HIV^+/impaired	6032	Frontal cortex
D2	HIV^+/HIVE/impaired	6800127569	Combined frontal lobe white matter/frontal cortex
D3	HIV^+/HIVE/impaired	7100107766	Combined frontal lobe white matter/frontal cortex
D5	HIV^+/HIVE/impaired	CA223	Frontal cortex

*All subjects are male.

Table 2

Human brain tissue sections used for immunohistochemistry**.

NNTC ID	HIV Positive	Primary Neurocognitive Diagnosis	Substance Use History	Drugs Used	Past/Current Use	Brain Region Examined
3013	No	Not assessed	Not assessed	Not assessed	Not assessed	Hippocampus
3022	No	Not assessed	Not assessed	Not assessed	Not assessed	Basal Ganglia
4135	Yes	Probable MCMD*	Yes	Multiple	Past and Current	Hippocampus
6065	Yes	Probable MCMD*	Yes	Multiple	Past	Basal Ganglia

* MCMD = Mild cognitive/motor deficit.

** All subjects are male.